Inkjet-Printed Three-Dimensional Colloidal Photonic Crystals for Structural Coloration of Solar Cells

INKJET-PRINTED THREE-DIMENSIONAL COLLOIDAL PHOTONIC CRYSTALS FOR STRUCTURAL COLORATION OF SOLAR CELLS

Roberto Speranza, Tommi Huhtamäki, Sakari Lepikko, Robin H. A. Ras, Janne Halme
Department of Applied Physics, Aalto University School of Science
P.O. Box 15100, 00076 Aalto, Finland

ABSTRACT: Large scale implementation of building-integrated photovoltaics (BIPV) requires matching the visual appearance of solar modules with other building materials. One approach is to add reflective color filters to conventional PV modules. Structural colors based on light interference are promising for this purpose, because they can produce color without parasitic light absorption, however, their angle-dependent (iridescent) appearance is unsuitable for most architectural applications and their fabrication methods ill-suited for color and pattern variation. Here, we report structural color filter fabricated by inkjet-printing three-dimensional photonic crystals (PC). A PC ink, consisting of monodispersed polystyrene nanoparticles of 200 nm diameter, was printed on a glass slide that had been treated with octadecyl-trichlorosilane (OTS) to control the droplet contact angle during drying, which was known to produce self-assembled 3-dimensional PC domes that exhibit angle-independent reflection. Measurements confirmed angle-independent cyan-colored reflection by the PC domes, but overall weak coloration. The PC color filter had 11.3 % peak reflectance at 467 nm, which caused 11 % decrease in the short-circuit current when coupled to a monocrystalline silicon solar cell. According to a theoretical analysis, increasing the surface coverage of the PC domes from 13 % to 80 % could increase the peak reflectance to 26 %.

Keywords: Building Integrated PV (BIPV), colorful solar cells, structural colors, photonic crystals, reflective colors

1 INTRODUCTION

Solar PV energy represents a reliable direction for clean energy production but still needs solutions to increase its market penetration. The IEA Photovoltaic Power Systems Program (PVPS) has identified five pillars that sustain the PV market penetration: the reduction of costs, an increase in technology efficiency and durability, innovation regarding energy storage systems and finally the level of integration of solar PV in buildings, the so-called Building-Integrated Photovoltaics (BIPV). The latter refers to all solutions aimed to make PV devices (modules, panels) more customizable in terms of size, shape and most importantly appearance: the goal is to realize multifunctional objects that can be 'integrated', rather than 'applied', in the design of a building, playing the role of both building materials and clean energy generating objects.

The ability to customize the appearance of solar panels is crucial in order to extend PV integration to the visible parts of the building envelope: facades, shading elements, windows. This trend is rapidly growing as more and more PV companies are offering solar panels with varied colors and textures. However, when the color of a standard solar panel is varied, a loss in power conversion efficiency is always observed so the goal is to reduce this effect as much as possible while maintaining the desired color hue and brightness [1]. An effective solution is to cover a conventional black solar panel with a wavelength-selective additional layer that maximizes the amount of radiation that reach the active part of the panel, reflecting only the wavelengths needed to form the desired color and at the same time minimizing parasitic light absorption [1-4]. Structural colors based on light interference in photonic crystals (PC) could be ideal for this purpose, because unlike pigments and dyes, they produce color without parasitic light absorption losses.

The light filtering properties of patterned PC have been largely investigated for application in displays, microfluidic and optical devices, anti-counterfeiting signatures, gas sensors and so on. Often, these structures have been fabricated combining the self-assembly properties of colloidal nanoparticles with the material deposition technique known as ink-jet printing [6-9]. Being the most common technique used to print digital images onto several substrates, by ink-jet printing it is possible to transfer customizable patterns on a wide range of substrates allowing an accurate control on the deposited material, but most importantly, it is suitable to be scaled to large area roll-to-roll fabrication processes [10-12].

Here, we report preliminary results from the fabrication of a structural color filter for solar by inkjet-printing three-dimensional photonic crystals. A reflective color filter fabricated this way could be used with all photovoltaic technologies, because it forms a separate semi-transparent photonic structure placed over the solar cell. Inkjet printing was chosen due to its accurate control of material deposition and possibility for multicolored pattern designs. A PC ink, consisting of monodispersed polystyrene nanoparticles of 200 nm diameter in a solution, was printed as individual droplets on a glass slide treated with octadecyl-trichlorosilane (OTS) by chemical vapor deposition (CVD). The surface treatment maintains high contact angle, which prevents the droplet from spreading and forces the nanoparticles to self-assemble to a dome-shaped, 3D photonic crystals that exhibit angle-independent reflective color, as demonstrated in earlier studies [15-17].

Measurements confirmed angle-independent cyan-colored reflection by the PC domes. The dome array printed glass reached 11.3 % peak reflectance at 467 nm and caused 11 % decrease in the short-circuit current density of an underlying monocrystalline silicon solar cell. Theoretical extrapolation of the results predicts that increasing the surface coverage of the PC domes from 13 % to 80 % could increase the peak reflectance to about 26 %. [2]

2 MATERIALS AND METHODS

2.1 Instruments and measurements

For material deposition a Fujifilm Dimatix Material Printer, model DMP-2850 was used. The machine allows to deposit many water-based, solvent, acidic or basic fluids on flat substrates, up to 25 mm thick, with a printable area of 210 mm x 260 mm. Each cartridge has 16 nozzles that deposit drops containing 10 pL of ink. The printed pattern can be designed with a Graphic User Interface (GUI), with a reported resolution of 100 dpi.

Optical images of the samples were acquired with a Leica DM4500 optical microscope to investigate the printing quality, the structural features and the angle-dependent optical behavior of the samples; the UR-Vis-NIR Agilent Cary 5000 spectrometer was used to perform spectrometry measurements on the printed materials.

The solar cells, integrated with the fabricated optical filter, were characterized with a QEX7 Solar Cell Spectral Response/Quantum Efficiency/IPCE Measurements System from PV Measurements, Inc. The external quantum efficiency (EQE) spectra and the short circuit current densities J_{sc} were collected.

2.2 Materials and preparation

The optical filter was made by a transparent substrate on top of which a pattern of three-dimensional colloidal photonic crystal aggregates were deposited as shown in **Figures 1 and 2**. Common transparent microscope glass slides were used as substrates. The slides were treated with octadecyltrichlorosilane (OTS) by chemical vapor deposition (CVD). The treatment was aimed to increase the contact angle of the substrate: advancing and receding contact angles (with respect to water) of 98° and 80° were measured, respectively.

The prepared printing ink was an aqueous solution of polystyrene nanoparticles. The nanoparticles were purchased by Polysciences, Inc. with a reported a diameter of 0.2 ± 0.01 µm. The particles were dispersed in a mixing solvent of water (60 wt%) and ethylene glycol (40 wt%), with a particle concentration or 10 wt%. Then the ink was treated ultrasonically and filtered with a 1.5 µm nylon mesh. The ink was then directly used to fill the printer cartridges.

The prepared ink was printed on the OTS treated substrates achieving a pattern of PC domes with a dome density of 53141 domes/cm^2 and a mean dome diameter of 18 ± 0.15 µm. Two successive prints with imposed dot spacing of 60 µm were performed, shifting the starting point for the second print by 30 µm in x and y directions. This was needed to avoid the merging of ink droplets due to impact behavior.

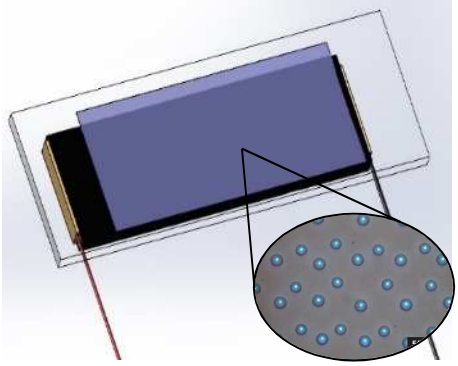

Figure 1: Three-dimensional model of the test device fabricated. A pattern of 3D photonic crystal domes (see insert) was inkjet-printed on an OTS-treated transparent glass substrate and put on top of a monocrystalline silicon solar cell.

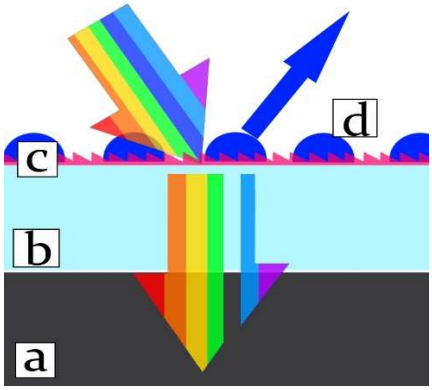

Figure 2: Schematic picture of the structure in section. The PC domes reflect a certain wavelength letting through the rest of the incoming radiation. (a) Solar cell, (b) glass substrate, (c) Octadecyltrichlorosilane (OTS), (d) Photonic crystal domes.

3 THEORY

3.1 Photonic bandgap position

Three-dimensional photonic crystals are highly ordered crystalline structures showing a periodic modulation of the refractive index in all three directions. When interacting with light, these structures show a behavior similar to the one showed by semiconductors with electrons: a photonic bandgap is observed, i.e. there is a certain band of wavelengths for which light cannot propagate through the material and is reflected back. The position of the stopband depend is usually derived by the Bragg condition for reflection, modified for the optical region, taking into account the refractive index [13]:

$$\lambda = 2d\sqrt{n_{\text{eff}}^2 - \sin\theta_{\text{i}}{}^2} \qquad (1)$$

Here λ is the bandgap position, d is the spacing between two crystalline planes, θ_{i} is the angle of incidence of incoming light, and n_{eff} is the effective refractive index calculated with the Bruggeman's relation [14]:

$$\phi_{\text{void}}\frac{n_{\text{void}}-n_{\text{eff}}}{n_{\text{void}}+(d_{\text{s}}-1)n_{\text{eff}}} + \phi_{\text{part}}\frac{n_{\text{part}}-n_{\text{eff}}}{n_{\text{part}}+(d_{\text{s}}-1)n_{\text{eff}}} = 0 \qquad (2)$$

Here ϕ_{void} and ϕ_{part} are the volume fractions of the material filling the void between particles and the volume fractions of the particles building the crystal, respectively. n_{void}, n_{part} and n_{eff} are the refractive indexes of the material filling the void, of the particles and the effective refractive index and d_{s} is the system dimensionality, in this case equal to 3.

3.2 Dome density

The optical behavior of the prepared optical filter was investigated also calculating the total reflectance of the printed samples integrated with the solar cell. This quantity was then related to the printed dome density and the dome coverage area. The total reflectance of the sample can be expressed approximately as:

$$R_{\mathrm{tot}} = \phi_{\mathrm{dome}} R_{\mathrm{dome-glass}} + (1 - \phi_{\mathrm{dome}}) R_{\mathrm{glass}} \quad (3)$$

Where R_{tot} is the total hemispherical reflectance, $R_{\mathrm{dome\text{-}glass}}$ is the reflectance of the dome-covered glass area and R_{glass} is the reflectance of the bare glass area. ϕ_{dome} is the fraction of the sample surface covered by the printed domes. With this approximation, it is possible to simulate the optical behavior of the sample considering printed patterns with a higher dome density corresponding to an increasing coverage fraction ϕ_{dome}.

An experimental value for the sample reflectance was calculated based on EQE measurements as:

$$R = 1 - T = 1 - \frac{\mathrm{EQE}}{\mathrm{EQE_{SiCell}}} \quad (4)$$

where R and T are the reflectance and transmittance, respectively, and EQE is the measured external quantum efficiency of the solar cell integrated with the optical filter and $\mathrm{EQE_{SiCell}}$ is the same in the case of the bare solar cell.

4 RESULTS AND DISCUSSION

4.1 Optical characterizations

The optical behavior of the filter was investigated measuring its total hemispherical reflectance. Here only the filter, not yet integrated with the solar cell, was considered. The results are shown in **Figure 3**:

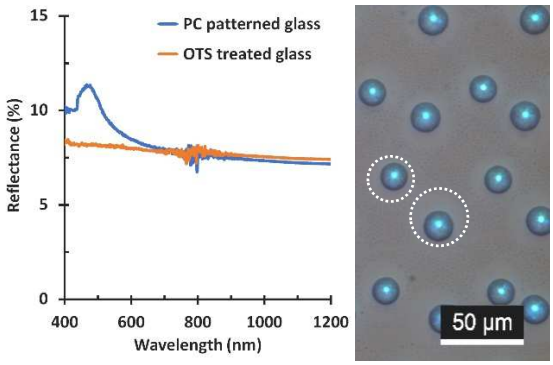

Figure 3: Left: Total hemispherical reflectance of the photonic crystal (PC) patterned glass and bare octadecyl-trichlorosilane (OTS) treated glass. The PC reflectance peak is at 467 nm. Right: Optical microscope image of the printed PC domes. The surface coverage of the domes was $5.31 \cdot 10^8$ domes/cm^2 and their mean diameter was 18 ± 0.15 µm. The dotted circles mark the initial droplet location before solvent evaporation and self-assembly of the PC dome, which appears as a brighter area due to the absence of small satellite droplets that cover the rest of the glass surface.

The optical stopband of the printed PC is clearly visible as a reflectance peak positioned at 467 nm, compared to the unpatterned glass slide that shown a flat, broadband reflection. The stopband position can be predicted from equation 1 by calculating the interplanar spacing d from a geometrical point of view as

$$d = \frac{2D}{\sqrt{6}} \quad (5)$$

where D is the diameter of the PC spheres building the crystal. Considering the angle of incidence θ_i equal to 0, as in normal incidence, and n_{eff} = 1.4 obtained from equation 2, the theoretical stopband position is 461 nm, which is close to the experimentally observed value.

Figure 3 shows an optical image of the printed PC domes. The microscopic appearance of the domes is very similar to other results reported in the literature when the domes are observed in normal reflection [15-17]: the center of the dome reflects a distinct color, in this case bright blue-cyan, in line with the position of the stopband within the visible spectrum. These results confirm that the inkjet-printed polystyrene nanoparticles self-assemble in a photonic crystal structure with a photonic stopband and visible reflection consistent with the Bragg's condition.

Figure 4 shows a photographic image of the solar cell covered by the coloring filter compared with the bare black silicon cell, and with the half-covered cell.

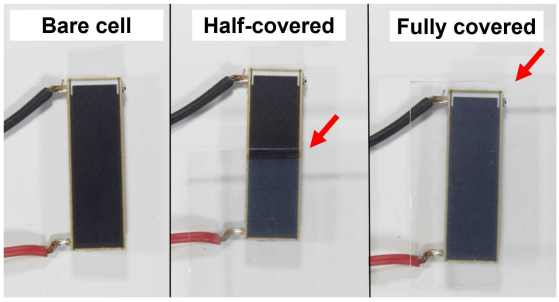

Figure 4: Photographs of the Si solar cell covered with the PC-patterned glass. The red arrow shows edge of the glass.

The coloring filter turns the appearance of the silicon cell from a dark black to a dark blue. The low brightness of the obtained color is in line with the results of the reflectance measurements and optical microscopic images: at the stopband, the reflectance peak is only 3 % higher compared to the bare glass value. The luminosity of the resulting color is further limited by the photopic sensitivity of the human eye at the stopband position 467 nm which is only 12 % compared to the peak sensitivity at 555 nm [19-20].

Figure 3 suggest that there is room to increase the area coverage by the PC domes on the glass slide, i.e. the dome density, which should lead to higher total PC layer reflectance and color brightness. This could be done in practice by increasing the number of multiple prints over the same area, however, droplets printed too close to each other were found to merge to a single larger dome during the solvent evaporation, which decreased the print uniformity, preventing systematic experimental study of this hypothesis. A speculative theoretical analysis was therefore carried out to scope the room for improvement.

With equation (3), we calculated the reflectance spectra as a function of the coverage area ϕ_{dome} and then obtained the RGB color coordinates corresponding to the obtained spectra, using the established methods of colorimetry [1]. **Figure 5** shows the colors corresponding to the calculated RGB coordinates. Increasing the coverage area from experimental value of 13 % to 80 %, the expected color shifts towards a more saturated cyan. Panel f in **Figure 5** shows the color corresponding to the reflection from the dome layer only, for ϕ= 13 %, obtained by eliminating the contribution of the glass substrate with equation 3: a significantly more saturated cyan is obtained, which is in line with the color observed in the microscopic images (**Figure 3**). This shows that the overall observed coloration potential of the PC domes layer is limited not

only by the dome density, but also by the broadband reflection from the substrate glass which tints the color towards grey.

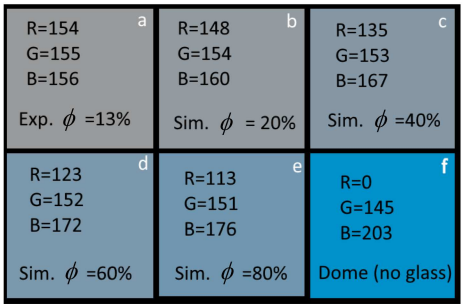

Figure 5: (a)-(e) RGB color coordinates corresponding to the measured ("Exp.") and predicted ("Sim.") total hemispherical reflectance of the PC-covered glass for different surface area coverage fraction by the domes (ϕ). (f) Same for the domes alone, for ϕ = 13 %, calculated by eliminating the effect of the reflectance form the glass substrate (equation 3).

The angle independence of the appearance of the coloring filter was investigated optically acquiring microscopic images of the samples at different tilting angles (**Figure 6**)

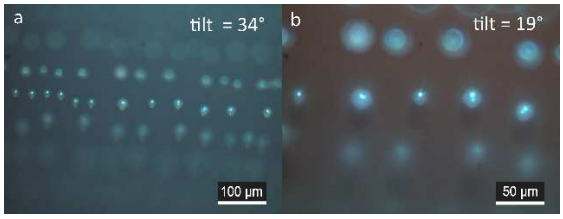

Figure 6: Optical microscope images of a tilted PC-patterned glass for (a) 34° and (b) 19° tilt angles.

Figure 6 shows that the same cyan color is observed at different tilting angles, suggesting that the PC domes reflectance and color is weakly dependent on the viewing angle, in agreement with previous studies [17-18]. **Figure 7** shows photographs of the solar cell covered with the coloring filter, at different tilting angles. Although the observable coloration is overall weak, as discussed above, we can see that even macroscopically, the optical appearance of the device does not change with angle, contrary to what normally happens with three-dimensional photonic crystals.

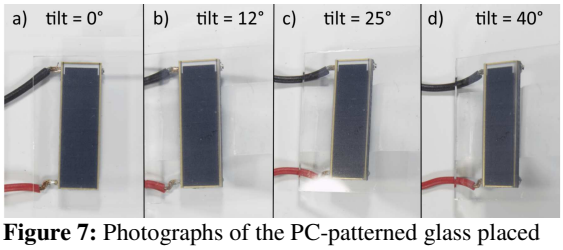

Figure 7: Photographs of the PC-patterned glass placed on top of the Si solar cell for different tilt angles.

4.2 Electrical characterization

The integrated device consisting of the monocrystalline silicon solar cell covered with the optical filter glass was characterized electrically by measuring the EQE and the short circuit current, which are the two most relevant figures-of-merit when considering the optical losses caused by the color filter on the solar cell. **Figure 8** shows the measured EQE data compared to the results obtained from the simulation at different dome coverage area, done with equation 4. The corresponding measured and simulated reflectance spectra are also reported in **Figure 8**.

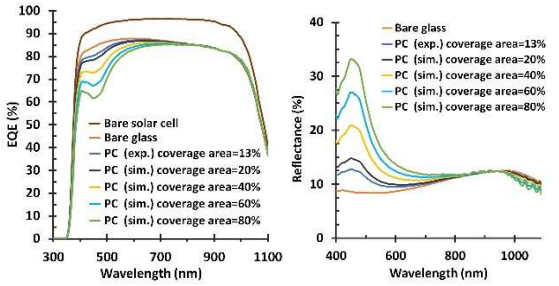

Figure 8: Left: measured ("exp.") and predicted ("sim.", using equations 3 and 4) EQE spectra of solar cell covered the PC crystal color filter glass, a bare glass, or as such (bare solar cell). Right: corresponding reflectance spectra approximated by equation 4.

It can be observed how the main optical losses are caused by the glass substrate that reduce the EQE values of around 9-13%. When the solar cell is covered with the PC color filter, a small EQE loss around the stopband position is observed, confirming that the optical filter acts only for the wavelengths needed to produce the desired color. Moreover, outside the stopband the parasitic absorption is nearly absent: the PC dome pattern is transparent to light outside the optical bandgap. The same is observed from the simulated spectra, i.e. increasing the coverage area the reflectance peak at the stopband increases, causing a deeper loss in the EQE.

The electrical short-circuit current performance of the fabricated colored solar device is summarized in **Table I** including predicted values for different dome coverage area. Here the peak reflectance value are referred to the filter (glass and printed PC) nonintegrated with the solar cell.

Table I: Measured and simulated short-circuit current performance of the monocrystalline silicon solar cell covered the PC crystal color filter glass, a bare glass, or as such (bare solar cell).

Dome coverage area (%)	Peak reflectance (%)	Simulated J_{sc} (mA/cm^2)	Measured J_{sc} (mA/cm^2)	ΔJ_{sc} (%)
Bare solar cell		39.0	38.9	
Bare glass		35.1	35.0	10
13	11.4	34.7	34.6	11
20	12.9	34.1		13
40	17.8	33.1		15
60	22.6	32.2		18
80	27.4	31.2		20

The optical filter, with a dome coverage area of 13 %, produce a peak reflectance, at the stopband, of 11.4 % causing a relative short circuit current loss of 11% with respect to the bare solar cell: this is only 1 % higher than the relative loss measured for the silicon cell covered with the unpatterned glass. From the simulation, it is expected that increasing the dome coverage area to 80 % the relative loss in the short circuit current density would be about 20 % with respect to the bare, on-covered solar cell.

5 CONCLUSIONS

We fabricated a reflective color filter by inkjet printing of three-dimensional photonic crystal for opaque colorful solar cells. A filter fabricated this way could be used with all photovoltaic technologies, because it forms a separate semi-transparent photonic structure placed over the solar cell. It shows a reflectance peak in the visible region, resulting in a colorful appearance with a nearly absent parasitic absorption outside the stopband position. The reflectance peak position depends on the crystalline structure of the printed domes and can be shifted by printing particles with different diameter. We printed polystyrene particles with a diameter of 200 nm obtaining a reflectance peak at 467 nm, which is located in the blue region, compared with the theoretical value of 461 nm predicted by equation 1.

The structure was realized by inkjet printing to allow for accurate control of material deposition and possibility for multicolored pattern designs. It was observed that a fundamental role is played by the optimization of inks properties such as viscosity, surface tension, presence of particle aggregates and so on. Inkjet printing allows also to deposit material without the need for vacuum, high temperature or controlled atmosphere in general.

We suggest that the saturation and brightness of the produced color can be increased by increasing the fraction of the printed area covered by the photonic crystal domes either increasing the dome density or increasing the dome dimension. Further tests in this direction will be fundamental to understand the real potential of this solution.

6 REFERENCES

[1] J. Halme, P. Mäkinen. Theoretical efficiency limits of ideal colored opaque photovoltaics, Energy & Environmental Science (2019).

[2] R. Speranza, Nanophotonic approaches to colourful solar cells and modules, Master's Thesis, Aalto University School of Science, (2018).

[3] Yifeng Chen, Yang Yang, Zhiqiang Feng, Pietro. P. Altermatt., Hui Shen, Color modulation of c-Si solar cells without significant current-loss by means of a double-layer anti-reflective coating, 27th European Photovoltaic Solar Energy Conference and Exhibition, (2012).

[4] S. Seo, L. J. Guo, K.-T. Lee, J. Y. Lee, Colored ultrathin hybrid photovoltaics with high quantum efficiency, Light: Science & Applications, 3:8e215, (2014).

[5] V. Neder, S. L. Luxembourg, A. Polman, Efficient colored silicon solar modules using integrated resonant dielectric nanoscatterers, Applied Physics Letters, 111(7):073902, (2017).

[6] A. C. Arsenault, D. P. Puzzo, I. Manners, G. A. Ozin, Photonic-crystal full-color displays, Nat. Photonics, 1, 468–472, (2007).

[7] C. Fenzl, T. Hirsch, O. S. Wolfbeis, Photonic Crystals for Chemical Sensing and Biosensing, Angew. Chem., Int. Ed., 53, 3318–3335, (2014).

[8] K. I. MacConaghy, C. I. Geary, J. L. Kaar, M. P. Stoykovich, Photonic Crystal Kinase Biosensor, J. Am. Chem. Soc., 136, 6896–6899, (2014).

[9] H. B. Hu, H. Zhong, C. L. Chen, Q. W. Chen, Magnetically Responsive Photonic Watermarks on Banknotes, J. Mater. Chem. C, 2, 3695–3702, (2014).

[10] P. Calvert, Inkjet Printing for Materials and Devices, Chemistry of Materials, 13 (10), 3299-3305, (2001).

[11] G. Perçin, B. T. Khuri-Yakub, Piezoelectric droplet ejector for ink-jet printing of fluids and solid particles, Review of Scientific Instruments 74, 1120, (2003).

[12] R. Abbel, P. Teunissen, E. Rubingh, T. van Lammeren, R. Cauchois, M. Everaars, J. Valeton, S. van de Geijn, P. Groen, Industrial-scale inkjet printed electronics manufacturing—production up-scaling from concept tools to a roll-to-roll pilot line, Translational Materials Research, Volume 1, Number 1, (2014).

[13] A. Reynolds, F. López-Tejeira, D. Cassagne, F. J. García-Vidal, C. Jouanin, and J. Sánchez-Dehesa, Spectral properties of opal-based crystals having SiO2 matrix, Phys. Rev. B, 60:11422–11426, (1999).

[14] M. Khardani, M. Bouaïcha, B. Bessaïs, Bruggeman effective medium approach for modelling optical properties of porous silicon: comparison with experiment, Physica Status Solidi (c) 4, No. 6, 1986–1990, (2007).

[15] J. Park, J. Moon, H. Shin, D. Wang, M. Park, Direct-write fabrication of colloidal photonic crystal microarrays by ink-jet printing, Journal of colloid and interface science, 298(2), 713-719, (2006).

[16] L. Cui, Y. Li, J. Wang, E. Tian, X. Zhang, Y. Zhang, & L. Jiang, Fabrication of large-area patterned photonic crystals by ink-jet printing, Journal of Materials Chemistry, 19(31), 5499-5502, (2009).

[17] M. Kuang, J. Wang, B. Bao, F. Li, L. Wang, L. Jiang, & Y. Song, Inkjet printing patterned photonic crystal domes for wide viewing-angle displays by controlling the sliding three phase contact line, Advanced Optical Materials, 2(1), 34-38, (2014).

[18] H. Gu, Y. Zhao, Y. Cheng, Z. Xie, F. Rong, J. Li, B. Wang, D. Fu, Z. Gu, Tailoring colloidal photonic crystals with wide viewing Angles, Small, 9, No. 13, 2266–2271, (2013).

[19] T. Smith, J. Guild, The C.I.E. colorimetric standards and their use, Trans. Opt. Soc., 33(3), 73, (1931).

[20] D. Malacara, Color Vision and Colorimetry: Theory and Applications, 2nd edn. SPIE, Bellingham, WA, USA, (2011).